

## **Double lock the COVID-19: inhibit SARS-COV-2 replication and suppress inflammation cytokine level by the golden compounds**

Zhesheng He<sup>2</sup>, Chunyu Zhang<sup>1</sup>, Zhongying Du<sup>1</sup>, Wencong Zhao<sup>1</sup>,  
Wenchao Niu<sup>1</sup>, Yucong Gao<sup>5</sup>, Yuhui Dong<sup>2</sup>, Jiadong Fan<sup>3</sup>, Bo He<sup>3</sup>, Peng  
Cao<sup>4</sup>, Huaidong Jiang<sup>+3</sup>, Yong Gong<sup>#2</sup>, Xueyun Gao<sup>\*1</sup>

1. Beijing University of Technology, Ping Le Yuan 100, Beijing, P. R. China. email: [gaoxy@ihp.ac.cn](mailto:gaoxy@ihp.ac.cn) <https://orcid.org/0000-0002-2267-9945>

2. Institute of High Energy Physics, Chinese Academy of Sciences, Beijing 100049, P. R. China

3. ShanghaiTech University, Shanghai 201210, P. R. China

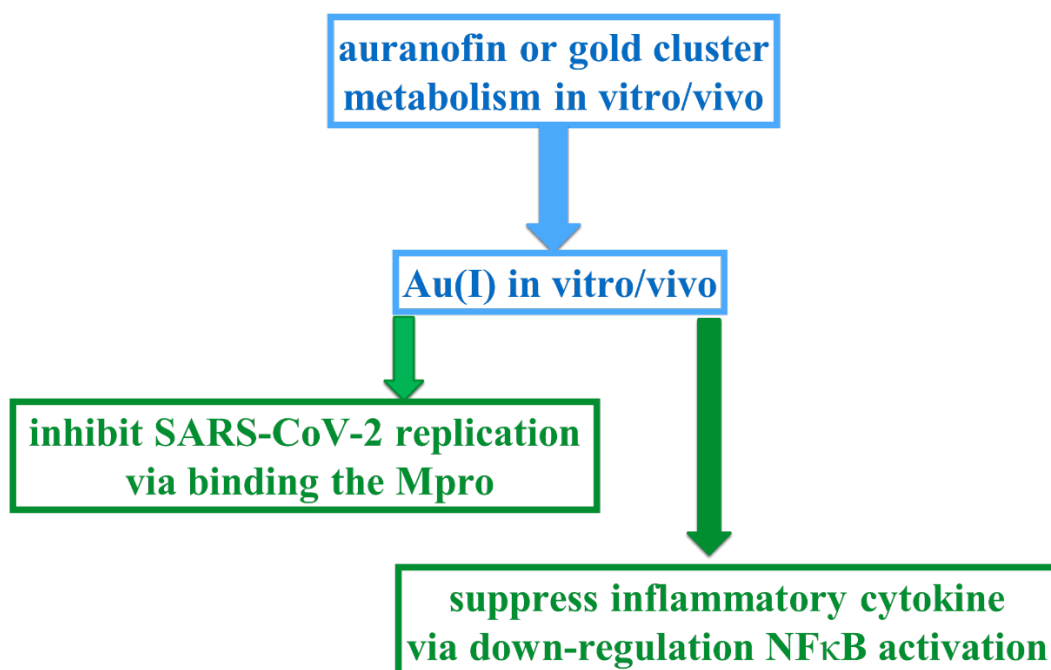
4. Peng Cao, National Laboratory of Biomacromolecules, Institute of Biophysics, Chinese Academy of Sciences, Beijing 100101, P. R. China. [peng@ibp.ac.cn](mailto:peng@ibp.ac.cn)

5. Yucong Gao, College of Engineering Civil, Environmental and Geodetic Engineering, The Ohio State University, Columbus, OH 43210 Ohio State University. [gao.1567@buckeyemail.osu.edu](mailto:gao.1567@buckeyemail.osu.edu)

**Corresponding Author: Huaidong Jiang, Yong Gong, Xueyun Gao**

**Abstract:** Our studies implied the golden compounds may be more effective against COVID-19 as they synergy inhibit SARS-COV-2 replication and down regulation inflammation cytokine level. Our crystal structure studies firstly revealed Au (I) ions, derived from auranofin (AF) or gold cluster (GA), covalently bind sulfur atom of Cys145 and Cys156 of M<sup>pro</sup> of SARS-COV-2. The auranofin or gold cluster well inhibit M<sup>pro</sup> activity in vitro. Auranofin or gold cluster could well suppress inflammation cytokine level of IL-6, IL-1 $\beta$ , TNF- $\alpha$  via down regulation NF- $\kappa$ B activation in macrophage. The cell viability and rat toxicity studies show gold cluster is more safety when compared FDA approved auranofin. The rat pharmacokinetic studies of gold cluster revealed its good bioavailability.

## **Double Lock the COVID-19 By Golden Drugs**



The COVID-19 pandemic is threatening human in the world now. There are more than 8 million COVID-19 patients and over 400,000s were dead by June 2020. To date, drugs treatment COVID-19 could somehow inhibit SARS-COV-2 replication or suppress inflammation cytokine level, but there is no drug to effectively treat COVID-19 (1, 2, 3, 4, 5). For example, Remdesivir could inhibit SARS-COV-2 replication in cell and animal studies (1, 2, 6). For severe COVID-19 patient, Remdesivir treatment was superior in shortening the time to recovery adult in hospital, but it was not associated with significant difference in viral load and clinical improvement of severe patient when compare with placebo treatment (3, 7). Recently, immune modulation drugs are applied to treat severe COVID-19, these drugs well reduce inflammation cytokine level and further down the mortality ratio of severe COVID-19 patient (4, 5, 8). However, these immunity modulation drugs could not inhibit SARS-COV-2 replication and decrease viral load in time which is desired for patient quickly recover. We hypothesize that if some novel compounds could synergy inhibit SARS-COV-2 replication and suppress inflammation cytokine level, they may make promising outcome for COVID-19 treatment in the world.

Actually we have done some researches before about a gold cluster named GA which is a lead compounds for rheumatoid arthritis treatment

(18, 20). According these results, we speculate gold compound , gold cluster or the FDA approved drug named Auranofin could suppress the inflammation cytokine level induced by SARS-COV-2. More interestingly, we have insight that the Au (I) derived from gold cluster or Auranofin might inhibit SARS-COV-2 replication by covalently binds Cys145 which is the key amino acid of the catalytic dyad of M<sup>pro</sup>.

Auranofin is FDA approved drug to treat rheumatoid arthritis (RA) disease via suppression inflammation cytokines level (9, 10). Auranofin could well down regulate inflammation cytokine such as IL-6, IL-1 $\beta$ , TNF- $\alpha$ , thus it is with potential to treat COVID-19 patients as these inflammation cytokines play important role to make COVID-19 more serious and induce mortality (11, 12, 13, 14). To date, if and how could auranofin inhibit SARS-COV-2 replication is not clear yet. It known that M<sup>pro</sup> play key role in SARS-COV-2 replication and small chemical compounds are screened to inhibit M<sup>pro</sup> via covalently bind the sulfur atom of Cys145 (15, 16). Previous reports discussed the Au (I) ion derived from gold compounds metabolism in vitro/vivo should be the active ingredient in RA treatment (17, 18). Following these data, we hypothesize Au (I) derived from gold compound are with strong potential to covalently bind the sulfur of Cys145, thus may inhibit M<sup>pro</sup> activity and further suppress SARS-COV-2 replication. To verify this insight, crystal structure of Auranofin or gold cluster complex with M<sup>pro</sup> are studied to

reveal if Au (I) could specifically bind Cys145 residues. As Auranofin side effects is some strong in clinical applications (19), gold cluster are used to compared with auranofin in this work. Gold cluster well suppress inflammation cytokine via down regulate the NF- $\kappa$ B activation and produce better outcome than Methotrexate (MTX) for RA treatment (18). More importantly it is with lower acute toxicity in rat when compared with FDA approved auranofin (18, 19). In case of gold cluster or auranofin could synergy inhibit SARS-COV-2 replication and suppress inflammation cytokine level, the gold cluster may be more acceptable in later preclinical studies owe to it safety.

In order to examine the structural basis of AF/GA functions in more detail, we determined the SARS-CoV-2 M<sup>pro</sup> crystal structures in the AF-treated form, the GA-treated form, and the native form without any compound treating as a control.

Generally speaking, the M<sup>pro</sup> structures with and without the drug-treating have a high similarity (Figure 1a , 1b and 2a), and also similar with the crystal structures of the SARS-CoV-2 M<sup>pro</sup>, which were determined most recently (15, 16). However, in the AF and GA treated structures, two densities of Au (I) ions were found clearly near to the residues of Cys145 and Cys156, and confirmed by the anomalous difference Fourier maps (Figure 1c and 1d) and the crystal X-ray fluorescence scan. They are defined as Au (I) 1 and Au (I) 2 here. It

indicates that the AF or GA can provide Au (I) ions to bind specific residues of M<sup>pro</sup> protein.

The overall structure of M<sup>pro</sup>-Au complex presents a homodimeric form (Figure 1a), with each monomer comprising three main domains, like those of other CoV Mpros, (Figure 1b). Domains I and II are  $\beta$ -barrels, which together resemble the chymotrypsin structure, and the active site of M<sup>pro</sup> is located in a cleft between them, whereas domain III are  $\alpha$ -helices mainly. Au (I) 1 was found the active pocket of M<sup>pro</sup>, and is coordinated by the side chain of Cys145. The key conserved residues Cys145 and His41 contribute to the catalytic dyad. Au (I) 2 was found at the outer area of M<sup>pro</sup>, and is coordinated by the side chain of Cys156. The temperature factors analysis show that the occupancy of two Au(I) ions is partial, indicating that the heavy atoms was introduced gradually.

Comparison of Au(I)-bound states with native state of M<sup>pro</sup> (Figure 2a) shows the introduce of Au ion does not induce the obvious protein structural conformation. The Au (I)1 ion is trapped in the active pocket (Figure 2b, c), indicating it would block the active site and also inhibit the catalytic function of the key residues of the catalytic dyad.

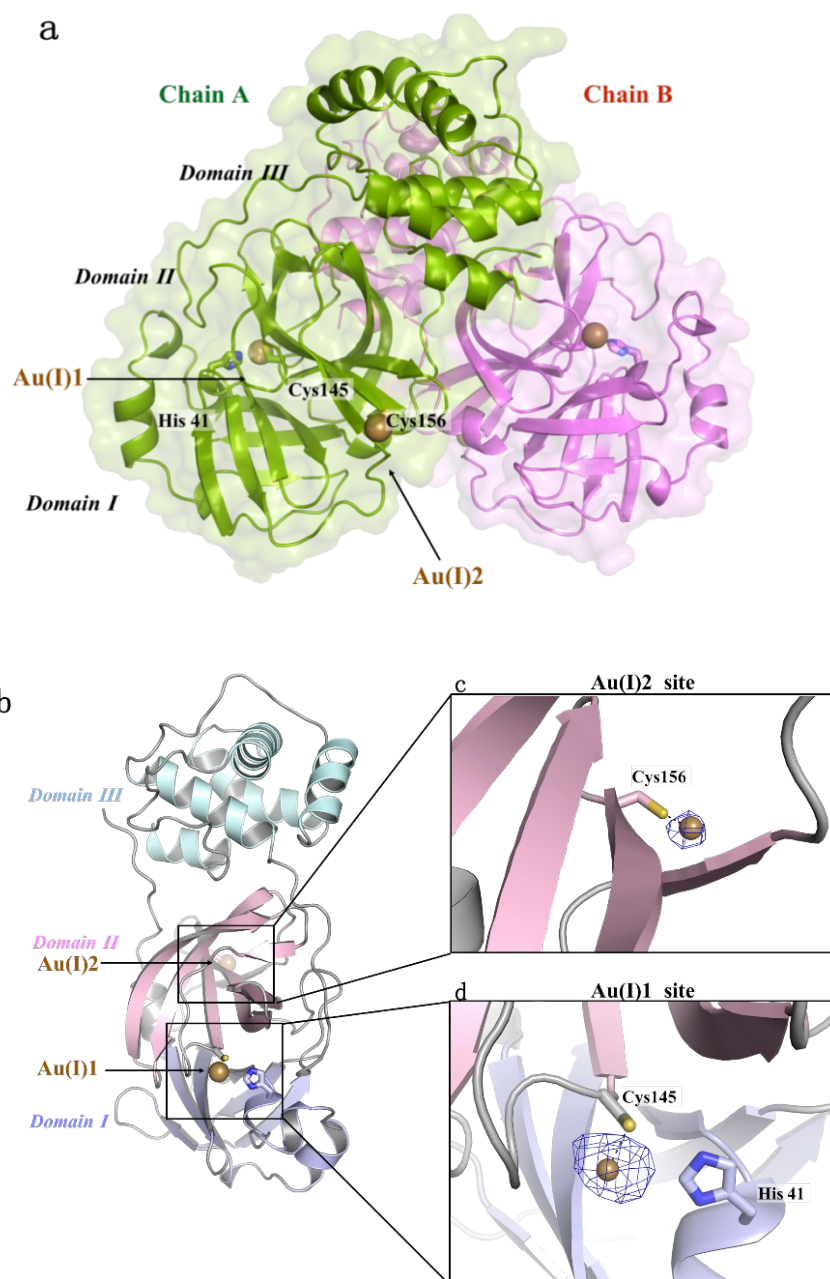


**Figure 1.** The X-ray crystal structure of  $M^{\text{pro}}$  in the AF/GA-treated Au-bound state. (a) The cartoon and surface presentation of  $M^{\text{pro}}$  homodimer with Chain A and Chain B colored in green and violet, respectively. (b) The cartoon presentation of one  $M^{\text{pro}}$  monomer with Domain I-III colored in lightblue, lightpink and palecyan. (c, d) The enlarged views of the Au(I)-bound sites. The anomalous difference Fourier maps (blue, contour at 5 sigma) are shown for Au(I)2 (c) and Au(I)1 (d). Domain I-III are labelled. The residues His41, Cys145 and Cys156 are shown in sticks and two Au ions in spheres.

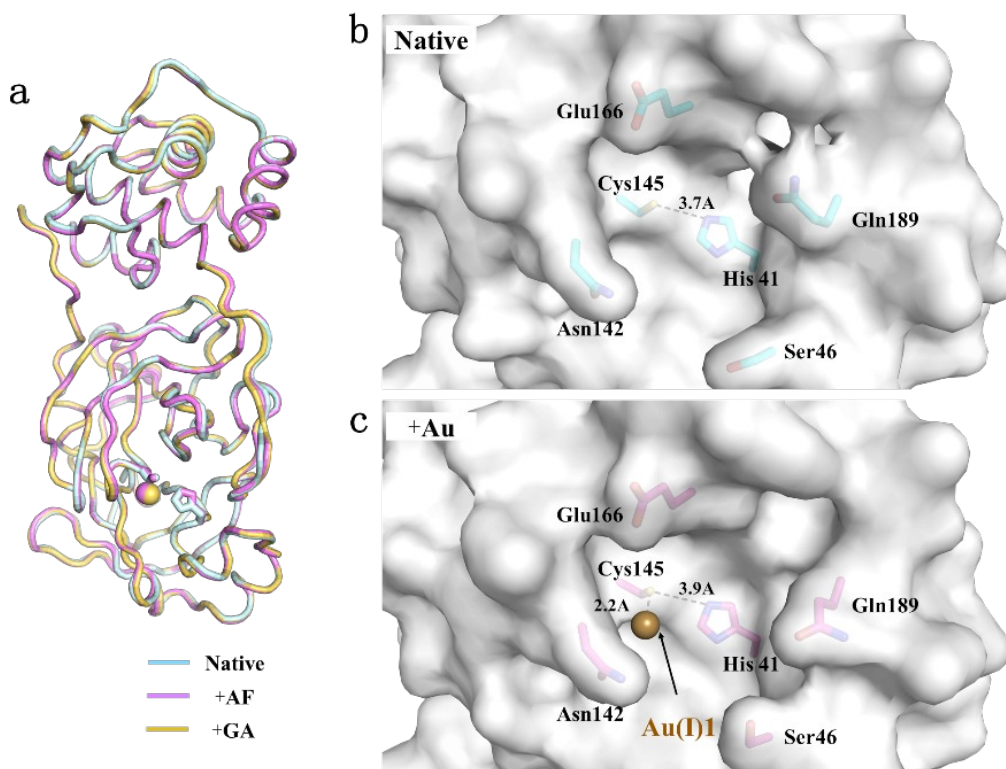


**Figure 2.** Comparison of Au(I)-bound state with native state of M<sup>pro</sup>. (a) Superposition of crystal structures of AF-treated (purple), GA-treated (yellow) and untreated M<sup>pro</sup> (blue). (b, c) The catalytic pocket of native (b) and Au(I)-bound M<sup>pro</sup> (b) in surface presentation and the surrounding residues in sticks. The distances between the two key residues of the catalytic dyad His41 and Cys145 are labelled.

To verify the auranofin or gold cluster could well inhibit M<sup>pro</sup> activity. The IC<sub>50</sub> of auranofin or gold cluster were carried out via the reported methods (15, 16, 21). In order to characterize M<sup>pro</sup> enzymatic activity, we used a fluorescence resonance energy transfer (FRET) assay (21). To do this, a fluorescence labeled substrate, (EDNAS-Glu)-Ser-Ala-Thr-Leu-Gln-Ser-Gly-Leu-Ala-(Lys-DABCYL)-Ser, derived from the auto-cleavage sequence of the viral protease was chemically modified for

enzyme activity assay.

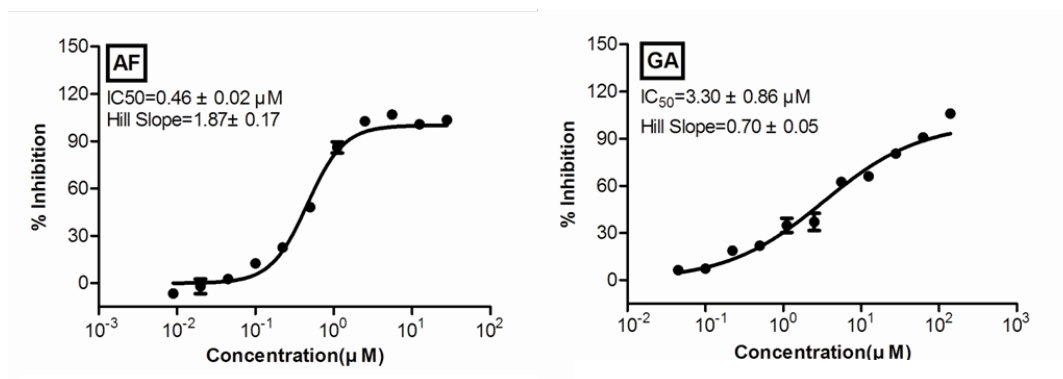


**Figure 3.** Inhibitions of M<sup>pro</sup> activity when it was exposed different auranofin or gold cluster, respectively. (a) IC<sub>50</sub> of Auranofin is ~0.46μM. (b) IC<sub>50</sub> of gold cluster is 3.30μM.

For inhibit M<sup>pro</sup> activity, IC<sub>50</sub> of Auranofin is about ~0.46μM and gold cluster is about ~3.30μM, respectively. Compared with IC<sub>50</sub> of reported compounds, the Auranofin is with very strong ability to inhibit M<sup>pro</sup> in vitro. Recently, Mukesh Kumar reported Auranofin could well inhibit SARS-CoV-2 replication in infected Huh cell and the EC<sub>50</sub> of Auranofin is about ~1.4μM, and they pointed that the inhibition of SARS-CoV-2 replication may be induced by gold suppress the thioredoxin reductase activity and induction of ER stress (22). According our crystal structure studies and M<sup>pro</sup> activity data, we provide direct proof that Au (I) derived from gold compound should play key role in SARS-CoV-2 replication in cell. Also, our data implied the gold cluster should inhibit SARS-CoV-2 replication as Au (I) derived from gold cluster also bind Cys145 and

Cys156 of M<sup>pro</sup> and well suppress its activity (**Figure 1, Figure 2, Figure 3**).

The toxicity features of these gold compounds are key parameters for their later studies in preclinical and clinical. We checked the gold compound toxicity in epithelial cell and macrophage cell lines as they play key roles in SARS-CoV-2 replication and inflammation cytokine production, respectively (9, 10, 11). For human bronchial epithelial cells (16HBE), the CC50 of Auranofin is about 0.6 μM while the gold clusters show no cell toxicity even if the dose increased to 100 μM in cell culture media (Figure 4a). And for macrophages (RAW264.7), the CC50 of auranofin is about 2.5 μM for RAW264.7 and gold clusters show no cell toxicity even if the dose increased to 100 μM in cell culture media (Figure 4b). For rat acute toxicity, the intraperitoneal LD50 for auranofin is ~25.5 mg/kg and the intraperitoneal LD50 for gold clusters is over ~288 mg/kg.bw (18, 23). For rat RA treatment, orally auranofin was used in a dose of 3 mg Au/kg.bw and intraperitoneal gold clusters were at 5 mg Au/kg.bw, such dose all well suppress inflammation cytokine levels in RA rats (17, 18, 19, 20). LD50/therapy dose is 8.5 for auranofin and over 57 for gold clusters. Previous reports showed there is no significant difference between gold cluster-treated rats (5 mg/kg.bw by intraperitoneal injection for 42 days) and control rats when checking the blood biochemical index, blood cell counts and histological analyses of main organs (18, 20). The

aforementioned cell toxicity and rat toxicity data all imply gold cluster are with more advantage in safety when consider gold compounds against COVID-19.

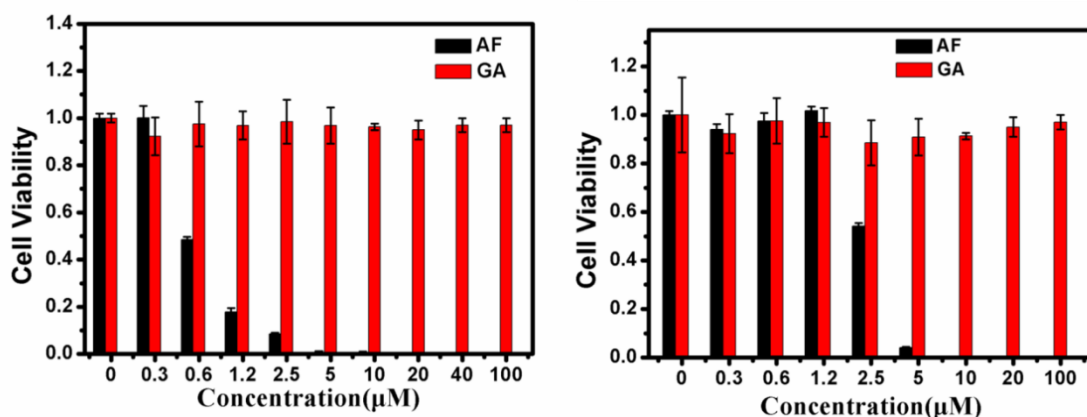


**Figure 4.** (a) Left images are 16HBE cell viability when cell exposed serial dose of AF or GA, respectively. (b) Right images are RAW264.7 cell viability when cell exposed serial dose of AF or GA, respectively.

When gold compounds are applied in preclinical studies or clinical application to against COVID-19, the bioavailability and tissue distribution is important parameter to be clarified firstly. The pharmacokinetic study of gold cluster via intraperitoneal injection, see **Table 1**. The basic kinetic characteristics of gold cluster in rats by ip injection at 5 mg/kg were as follow. According to the parameters calculated by statistical moments, the values of  $T_{max}$  for gold cluster in male or female rats were 2 hours and the values of  $C_{max}$  for gold cluster in male or female rats were 29.99μg/mL or 31.750μg/mL, respectively. The

values of  $t_{1/2z}$  for gold cluster in male or female rats were 21.626 h or 11.068 h respectively. The values of bioavailability (F) for gold cluster in male or female rats were 92.06% or 96.41%, respectively, based on the data analysis of iv injection (**Table 2**). This data confirmed gold cluster is with very good bioavailability in vivo. In our previous report, after 42 days intraperitoneal gold cluster of 5mg/kg.bw for RA rat model, there is 0.03mg Au/g in brain, 0.05mg Au/g in lung, 0.1mg Au/g in heart, 0.2mg Au/g in liver, 0.23mg/g in spleen, 0.45mg/g in kidney (18). As clinical reports revealed COVID-19 trigger inflammation cytokine storm and damage organs and result their function failure for severe patient (4, 5, 9, 10, 11). The gold components well distribute in important organs like lung, heart, liver, kidney, brain, and spleen are beneficial in COVID-19 treatment as they could inhibit SARS-COV-2 replication and suppression inflammation cytokine level therein.

**Table 1. Rat intraperitoneal injection 5 mg Au/kgbw of gold cluster**

| parameter           | unit   | value         |             |
|---------------------|--------|---------------|-------------|
|                     |        | ip01 (Female) | ip02 (Male) |
| $AUC_{(0-t)}$       | mg/L*h | 533.680       | 509.615     |
| $AUC_{(0-\infty)}$  | mg/L*h | 599.607       | 785.906     |
| $A_{\mu}MC_{(0-t)}$ |        | 6371.497      | 7609.285    |

|                        |        |          |           |
|------------------------|--------|----------|-----------|
| $A\mu MC_{(0-\infty)}$ |        | 9797.793 | 26177.773 |
| $MRT_{(0-t)}$          | h      | 11.939   | 14.931    |
| $MRT_{(0-\infty)}$     | h      | 16.340   | 33.309    |
| $VRT_{(0-t)}$          | $h^2$  | 83.183   | 123.090   |
| $VRT_{(0-\infty)}$     | $h^2$  | 258.916  | 1045.121  |
| $t_{1/2z}$             | h      | 11.068   | 21.626    |
| $T_{max}$              | h      | 2        | 2         |
| $CL_z/F$               | L/h/kg | 0.008    | 0.006     |
| $V_z/F$                | L/kg   | 0.133    | 0.199     |
| $C_{max}$              | mg/L   | 31.750   | 29.990    |
| F                      | %      | 96.407   | 92.060    |

**Table 2. Rat Intravenous injection 5 mg Au/kgbw of gold cluster**

| Parameters          | Unit   | Parameter value |           |
|---------------------|--------|-----------------|-----------|
|                     |        | iv 01 (F)       | iv 02 (M) |
| $AUC_{(0-t)}$       | mg/L*h | 641.972         | 465.165   |
| $AUC_{(0-\infty)}$  | mg/L*h | 823.672         | 556.880   |
| $AUMC_{(0-t)}$      |        | 8616.252        | 5459.131  |
| $AUMC_{(0-\infty)}$ |        | 19606.123       | 10532.811 |
| $MRT_{(0-t)}$       | h      | 13.422          | 11.736    |
| $MRT_{(0-\infty)}$  | h      | 23.803          | 18.914    |
| $VRT_{(0-t)}$       | $h^2$  | 110.213         | 91.859    |
| $VRT_{(0-\infty)}$  | $h^2$  | 598.942         | 399.534   |
| $t_{1/2z}$          | h      | 16.967          | 13.389    |
| $CL_z$              | L/h/kg | 0.006           | 0.009     |
| $V_z$               | L/kg   | 0.149           | 0.173     |

In conclusion, gold compounds are with strong potentials to be the specific effective drug to treat COVID-19 in the world. The Au (I) metabolism from gold cluster or FDA approved auranofin could covalently bind with Cys145 and Cys156 of SARS-CoV M<sup>pro</sup> to inhibit its activity in vitro. The gold cluster and auranofin all could well suppress NF $\kappa$ B activation to down-regulation of inflammation cytokine level of

IL-6, IL-1 $\beta$ , TNF- $\alpha$  in macrophage cell and rat RA model. Compared with auranofin, gold cluster is with more advantage in toxicity when consider later preclinical study against COVID-19.

## Reference

1. Sheahan et al., Sci. Transl. Med. 2020, 12, eabb5883
2. Brandi N. Williamson et al, Nature 2020,  
<https://doi.org/10.1038/s41586-020-2423-5>
3. Yeming Wang et al., Lancet 2020, 395, 1569, 1578
4. Yang Cao et al., Journal of Allergy and Clinical Immunology 2020,  
<https://doi.org/10.1016/j.jaci.2020.05.019>
5. Mark Roschewski<sup>1</sup> et al, Science Immunology 2020, DOI:  
10.1126/sciimmunol.abd0110
6. Andrés Pizzorno et al. bioRxiv preprint 2020,  
<https://doi.org/10.1101/2020.03.31.017889>
7. Beigel et al, The New England Journal of Medicine 2020, DOI:  
10.1056/NJEMoa2007764
8. Giacomo De Luca et al., The Lancet 2020,  
[https://doi.org/10.1016/s2665-9913\(20\)30170-3](https://doi.org/10.1016/s2665-9913(20)30170-3)
9. Finkelstein, A. E. et al., Annals of the Rheumatic Diseases 1976, 35,  
251-257.

10. John R. Warda et al., *Arthritis and Rheumatism* 1983, 26(11), 1303-1315
11. Michele Catanzaro et al, *Signal Transduction and Targeted Therapy* 2020, 5, 84
12. Matthew Zirui Tay et al., *Nature Reviews Immunology* 2020, 20, 363–374
13. Miriam Merad et al., *Nature Reviews Immunology* 2020, 20, 355-362
14. Georg Schett et al., *Nat. Rev. Rheumatol.* 2020, <https://doi.org/10.1038/s41584-020-0451-z>
15. Zhenming Jin et al., *Nature* 2020, 582, 289–293.
16. Linlin Zhang et al., *Science* 2020, DOI: 10.1126/science.abb3405
17. W. F. Kean, *British Journal of Rheumatology*, 1997, 36, 560-572
18. Fuping Gao et al, *Adv. Sci.* 2019, 6, 1801671-1801684
19. Cerner Multum, 2019, <https://www.drugs.com/mtm/auranofin.html>
20. Qing Yuan et al, *ACS Omega* 2019, 4, 9, 14092-14099
21. V. Grum-Tokars et al., *Virus Research* 2008, 133, 63–73
22. Hussin A. Rothan et al., *bioRxiv preprint* doi: <https://doi.org/10.1101/2020.04.14.041228>
23. Cayman Chemical, *Safety Data Sheet of Auranofin* 2018, <https://www.caymanchem.com/msdss/15316m.pdf>

## **Supporting data**

## **Cloning, expression and purification of SARS-CoV-2 M<sup>pro</sup>**

The full-length gene encoding SARS-CoV-2 M<sup>pro</sup> was optimized and synthesized for Escherichia coli (E. coli) expression (GENEWIZ). Then the gene was cloned into a modified pET-28a expression vector with an N-terminal (His)<sub>6</sub>-tag followed by a Tobacco etch virus (TEV) cleavage site. The construct was confirmed by DNA sequencing. The plasmid was further isolated and transformed into the Escherichia coli Rosetta (DE3) expression strain (Invitrogen). The cells containing the plasmids above were grown to an OD<sub>600</sub> =0.8 and induced with isopropyl β-D-thiogalactopyranoside (IPTG) to a final concentration of 0.5mM at 16 °C for 14 h.

Cells were then harvested by centrifugation at 4600g, resuspended in lysis buffer (120mM Tris/HCl, pH 8.0, 20 mM imidazole and 300 mM NaCl) and lysed by French press, the lysate was centrifuged at 15 000 g for 50 min. Then the supernatant was loaded on to a Ni-NTA column pre-equilibrated with lysis buffer, and washed with 20 mM Tris/HCl, pH 8.0, 300 mM NaCl and 50 mM imidazole. The protein was eluted in 20 mM Tris/HCl, pH 8.0, 150 mM NaCl and 300 mM imidazole. TEV protease was added to the His tag fused protein and dialyzed overnight into anion-exchange chromatography buffer A (20mM Tris/HCl, pH8.0, 20mM NaCl, 1mM DTT, 1mM EDTA). The protein was further purified using a Resource-Q column of AKTA fast protein liquid chromatography (GE

Healthcare) by elution with a linear gradient of 20-500 mM NaCl ,20 mM Tris/HCl , 1mM EDTA , 1mM DTT and pH 8.0. The purity was analysed by SDS/PAGE at each step. The purified and concentrated SARS-CoV-2 M<sup>pro</sup> was stored in 20mM Tris-HCl(pH7.3), 20mM NaCl , 1mM DTT, 1mM EDTA at -80 for enzyme activity assays and crystallization.

### **Crystallization, data collection and structure determination**

M<sup>pro</sup> crystallization screening was carried out at 22 °C using the sitting-drop vapor-diffusion technique that 0.7µl 6mg/ml protein solution mixed with an equal volume of reservoir solution. Initial crystals were found under the crystallization conditions of the PEG/Ion Screen Kit in Crystal Screen (Hampton Research). After optimization, the best crystals of M<sup>pro</sup> were obtained under the condition of 200mM KF and 15% PEG 3350 after 4–5 d. Crystals of M<sup>pro</sup> were soaked in reservoir solutions plus 10mM AF or GA for 15hr.

Prior to data collection, all crystals were cryo-protected by plunging them into a drop of reservoir solution supplemented with 10–20% glycerol, then flash frozen in liquid nitrogen

The initial phase was determined by molecular replacement method using the program Phaser from CCP4 program suit, with the crystal structure of COVID-19 main protease in complex with an inhibitor N3 (PDB entry 6LU7)

as the initial model. The refinement was carried out using Phenix and Refmac, model building was carried out by COOT, and MolProbity was used to validate the structure. The locations of Au (I) ions were identified according to the anomalous difference Fourier maps. Data collection and refinement statistics are listed in Table S1. The structural figures were prepared using using PyMOL (<http://www.pymol.org>).

Table S1. Data collection and refinement statistics

---

| $M^{\text{pro}}$ -AF treated | $M^{\text{pro}}$ -GA | Native |
|------------------------------|----------------------|--------|
|------------------------------|----------------------|--------|

---

| <b>Data collection</b>                              |                                  |                                  |                                  |
|---|----------------------------------|----------------------------------|----------------------------------|
| Wavelength (Å)                                      | 0.86                             | 0.98                             | 0.98                             |
| Space group   | C2                               | C2                               | C2                               |
| Cell dimensions                                     |                                  |                                  |                                  |
| <i>a</i> , <i>b</i> , <i>c</i> (Å)                  | 114.3, 54.0, 44.7                | 113.8, 53.8, 44.6                | 113.8, 54.0, 44.8                |
| $\alpha$ , $\beta$ , $\gamma$ (°)                   | 90.0, 101.8, 90.0                | 90.0, 102.0, 90.0                | 90.0, 101.3, 90.0                |
| Resolution (Å)                                      | 50-2.84 (2.87-2.84) <sup>a</sup> | 50-1.72 (1.75-1.72) <sup>a</sup> | 50-1.80 (1.83-1.80) <sup>a</sup> |
| <i>R</i> <sub>merge</sub>                           | 0.087 (0.136)                    | 0.089 (0.823)                    | 0.062 (0.633)                    |
| $\langle I/\sigma(I) \rangle$                       | 16.4 (8.2)                       | 33.8 (2.2)                       | 27.0 (2.0)                       |
| Completeness (%)                                    | 98.6 (92.0)                      | 99.8 (100.0)                     | 99.3 (98.5)                      |
| Redundancy  | 5.6                              | 6.2                              | 6.4                              |
| <b>Refinement</b>                                   |                                  |                                  |                                  |
| Resolution (Å)                                      | 50-2.84                          | 50-1.72                          | 50-1.80                          |
| No. reflections                                     | 6,023                            | 27,939                           | 23,287                           |
| <i>R</i> <sub>work</sub> / <i>R</i> <sub>free</sub> | 0.197/0.236                      | 0.199/0.247                      | 0.211/0.264                      |
| No. atoms   |                                  |                                  |                                  |
| Protein   | 2,329                            | 2,329                            | 2,329                            |
| Au  | 2                                | 2                                | 2                                |
| Water   | 97                               | 209                              | 200                              |
| B-factors   | 33.8                             | 37.3                             | 24.3                             |
| Rmsd bond length (Å)                                | 0.006                            | 0.010                            | 0.008                            |
| Rmsd bond angle (°)                                 | 1.3                              | 1.1                              | 1.2                              |
| Ramachandran Plot                                   |                                  |                                  |                                  |
| Favoured (%)  | 97.3                             | 97.7                             | 98.3                             |
| Allowed (%)   | 2.7                              | 2.3                              | 1.4                              |
| Outliers (%)  | 0.0                              | 0.0                              | 0.3                              |

<sup>a</sup> The values in parenthesis mean those of the highest resolution shell.